The International Journal of Advanced Manufacturing Technology
https://doi.org/10.1007/s00170-020-05348-0

ORIGINAL ARTICLE

Stress-induced stabilization of pyrolyzed polyacrylonitrile and carbon nanotubes electrospun fibers

Paola Serena Ginestra [1] · Elisabetta Ceretti [1]

Received: 27 June 2019 / Accepted: 17 April 2020

Abstract
The unique properties of graphitic carbons have gained widespread attention towards their development and application. Carbon materials can be synthesized by thermal decomposition and, more specifically, carbon pyrolysis from polymer precursors. The paper shows the pyrolysis process of polyacrylonitrile (PAN) in the presence of multi-walled carbon nanotubes (MWCNTs) according to different manufacturing process conditions. The electrospinning process of the PAN-MWCNTs solution on multi-plates collectors was firstly analyzed. The morphology and the particles arrangement of the electrospun fibers was studied under scanning and transmission electron microscopes. Moreover, the composite fibrous mats were characterized by RAMAN spectroscopy to identify the effects of a mechanical tension application during the thermal stabilization phase performed before the pyrolysis treatment to obtain carbon fibers from the precursor polymer. The results show that the graphitization of the pyrolyzed fibers is enhanced by the combination of MWCNTs and a mechanical stress applied during the thermal treatment.

Keywords Electrospinning · Carbon · Nanomanufacturing · Pyrolysis

1 Introduction

Polymer fibers are used for diverse applications. According to the last estimates, the world consumption of fibers is reaching 60 million tons per annum [1, 2]. Polymer nanofiber networks are being considered as filters, scaffolds for tissue engineering, protective clothing, reinforcements in composite materials, and sensors [3–5]. Although some of these applications are in the development stage, a few have been commercially exploited [6]. Carbon-based materials have gained interest for the attractive electronic and structural properties and the intrinsic electrochemical stability useful for a variety of technological applications. A carbon fiber (CF) is defined as a fiber containing at least 92 wt% of carbon, while a fiber containing at least 99 wt% carbon is usually called a graphite fiber [7]. Almost all CFs are produced from pyrolysis of precursor fibers. The current carbon fiber market is dominated by polyacrylonitrile (PAN) carbon fibers, while the rest is related to pitch carbon fibers and a very small amount of rayon carbon fiber textiles [8, 9]. The optimization of the pyrolysis process of the PAN precursor fibers would ideally result in enhanced performances of the resulting CF [10, 11]. Pyrolytic carbon fibers are chemically stable and exhibit a wide potential window but require post-processing to be effective especially in sensing applications. Nanoparticles can change the structural and physical properties of the fibers as reinforcement agents. The most used nanoparticles to reinforce nanofibers are carbon nanomaterials and especially nanotubes and graphene [12]. The growing expansion of new carbon materials resulted in an expansion of the theoretical research on the correlation between the microstructural changes induced by these nanoparticles and the synthesis of carbon-enriched materials [13, 14]. Carbon nanotubes (CNTs) and graphene nanosheets have been studied in the last two decades and a lot of research has been focused on these two carbon allotropes combined with polymer nanocomposites [15]. However, the production of carbon-based materials with tailorable properties has still to be fully understood despite their continuous industrial use. On the other hand, the production of carbon substrates, such as electrodes, is challenging due to the expensive costs of the fabrication. Moreover, the relationship between the synthesis and structure of new carbon materials is still uncertain despite their widespread use in industry. Anyhow, CFs possessing high degree of preferred orientation of the graphene layers

✉ Paola Serena Ginestra
paola.ginestra@unibs.it

[1] Department of Mechanical and Industrial Engineering, University of Brescia, V. Branze 38, 25123 Brescia, Italy

Published online: 11 May 2020

are known to exhibit optimal properties in terms of electrical and thermal conductivity and promising mechanical properties.

Here, the authors demonstrate how the effects of a mechanical treatment can significantly enhance the precursor fibers graphitization by the specific rearrangement of the organic material in relation to CNTs. The aim of the study was to understand whether PAN fibers may be graphitized at a lower pyrolysis temperature compared to the commercially available PAN-based CFs [16], challenging the present approaches concerning the graphitization of polymers. Carbon composites have extensively been developed using PAN fibers heat-treated to temperatures between 1000 and 2500 °C [17]. The overall structure of PAN-based carbon fibers remains that of a hard carbon, thus non-graphitic, till 2000 °C, and the transformation of the structure into a graphitic carbon, usually derived from soft carbon, is achieved above 2500 °C. The reduction of the temperature required to obtain graphitic carbon from a polymer precursor is therefore crucial to spread the application of this technique. The graphitization of organic precursor has been attributed to their chemical and physical properties that can prevent the formation of graphitic planes without a rearrangement of the carbon atoms in the fusion phase occurring during the heat treatment. Subsequently, alternative strategies are being investigated to induce graphitization in polymer precursors [18]. In this work, the electrospinning process of PAN enriched with multi-walled CNTs was used to enhance the orientation of the precursor's chains that was preserved with the application of a mechanical stress during the thermal stabilization prior to pyrolysis. The extent of graphitization of PAN-CNTs fibers is found to be dependent on the fibers-nanoparticles interactions [19]. Previous works already focused on the characterization of PAN-CNTs electrospun fibers. The glass transition temperature (T_g) of PAN fibers can be modified by 3 °C with the insertion of CNTs due to the reduction of mobility of the PAN chains [20, 21]. In particular, an increase of the Tg of PAN-CNTs fibers has been observed by incorporating 0.75 wt% of CNTs into the PAN matrix but the Tg increasing trend is reduced at higher CNTs contents due to a progressive lower interaction between the nanoparticles and the polymer chains. Moreover, the chemical composition, before and after carbonization, of PAN-CNTs fibers has been deeply investigated [22] showing that the addiction of CNTs contributes to orient the crystallization of the PAN molecular chains during the spinning process leading to a higher crystal perfection of the PAN polymer in the PAN-CNTs composite. These results highlighted the potential role of the CTNs as a template to maintain the polymer extended chain configuration during carbonization [23].

The nanoparticles arrangement was evaluated under EDS, TEM (HRTEM; FEI, Titan 80–300 kV S/TEM), and RAMAN spectroscopy (Renishaw InVia Raman Microscope), while the effects of the mechanical tension during thermal stabilization prior to the pyrolysis treatment were analyzed and characterized by RAMAN spectroscopy and SEM (Hitachi Regulus 8230 ultra-high resolution SEM).

2 Electrospinning and pyrolysis

The first step for the production of the electrospinning solution is the suspension of 1% MWCNTs (diameter of 110–170 nm, length 5–9 μm) in dimethylformamide (DMF) followed by sonication for 1 h at 35 °C. Three homogeneous solutions of 8 wt% of PAN (150,000 g/mol) were prepared by adding the polymer to the MWCNTs solution as previously reported [24, 25]. The MWCNTs-PAN solution was then stirred for 48 h at 30 °C. The electrospinning tests were carried out with the newly formulated solutions and the collected fibers were characterized to analyze the interaction between the nanotubes and the polymer. The electrospinning was carried out by applying a flow rate of 0.8 ml/h to a 10-ml syringe equipped with a 21 Gauge needle. The voltage applied between the needle and the collector was 12 kV and the distance between the needle tip and the collector was kept at 210 mm. Furthermore, two different copper collectors were used: one single square collector and a multi-plates collector. The geometry of the collector can have a strong influence on the deposition of the fibers according to the direction of the electrical field. In this context, a multi-plates collector allows the alignment the fibers along one parallel direction by the generation of an ordered electric field towards the plates [26, 27]. On the other hand, the fibers are randomly deposited on the square collector due to the uniformity of the electrical field on the grounded collector. The process was run for 30 min and the tests were performed at ambient conditions of 25 °C and relative humidity of 40% [1]. The obtained fibers were then thermally stabilized prior to the carbonization (Fig. 1). Since the heating rate determines the evolution rate of volatile components from PAN fibers and consequently affects the performance of the carbon fibers, a temperature of 280 °C was applied for 6 h. The samples stabilized are then submitted to carbonization in a nitrogen environment at an approximate flow rate of 4600 sccm in order to remove all the non-carbon elements and obtain fibers made by pristine carbon [28]. The temperature and the time of exposure in this step are as fundamental as for the stabilization.

The temperature, starting from 20 °C (room temperature), is increased for 60 min until it reaches 300 °C, so the ramp is 4 °C/min. Then, the temperature is maintained for 60 min at 300 °C to complete the preliminary stage of the process of the pre-carbonization. At this point, the temperature is increased again until the temperature achieves 1050 °C: the ramp in this case is 2.5 °C/min [29]. During this step, the second and the final stages of the process of the pre-carbonization are carried out.

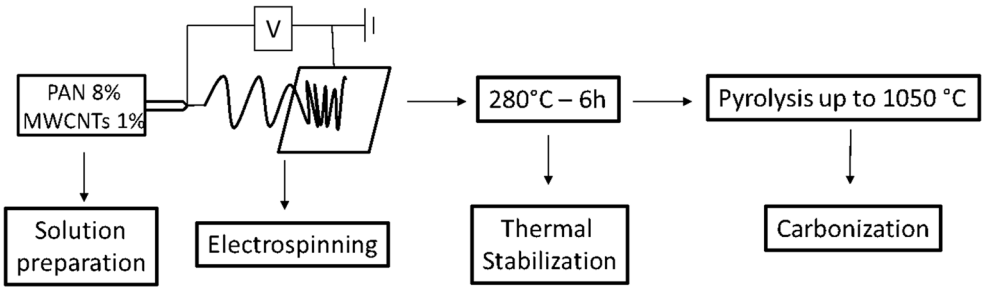

Fig. 1 Schematic illustration of the micro fabrication process of the pyrolyzed electrospun fibers

When the temperature reaches 1050 °C, the process of carbonization takes place and the temperature is kept constant for 60 min in order to finish the process. All the analyses presented in the following sections have been carried out on pyrolyzed samples.

2.1 MWCTNs-PAN fibers

The elemental composition of the MWCNTs-PAN samples obtained on the square collector was analyzed with SEM-EDS mapping as shown in Fig. 2.

The quantitative elemental composition of the MWCNTs-PAN fibers before (Fig. 2a) and after (Fig. 2b) pyrolysis reveals the presence of oxygen due to the chemical reactions occurring during the stabilization of PAN as a carbon fiber precursor [30]. The variation of the nitrogen content can be attributed to the polyacrylonitrile composition $(C_3H_3N)_n$ that is carbonized by pyrolysis carried out in a controlled nitrogen atmosphere.

The distribution and arrangement of the MWCNTs was analyzed under TEM operating at 300 kV. Figure 3a shows that MWCNTs-PAN samples have no porosity or other defects, except for a small surface roughness. The examination of the lattice fringes in the micrographs shows the effects of the carbon microstructures on the fibers developed by the electrospinning process. The MWCNTs-PAN selected area of the diffraction pattern, taken from a thin area of the fibers network, shows concentered circles that are formed from multiple sets of six-fold-symmetrical spots (Fig. 3b). This pattern is due to multi-layers of sp2 hybridized carbon planes (from MWCNTs and/or grown carbon crystals) with random orientation with respect to the incident electron beam. MWCNTs-PAN fibers present a multi-layer wall of the carbon nanotube and some initial ordering in the shell region near the surface of the nanofiber. This can be better noticed from Fig. 3c in which a detail of the fiber's microstructure is shown.

Close to the surface (a), it is possible to distinguish the orientation of the fringes that indicates a good alignment of the MWCNTs along the fiber axis, while in the core (b), the crystals are randomly oriented. This demonstrates the well-known distinction between the core and shell regions on PAN-precursor nanofibers. The distance between the fringes

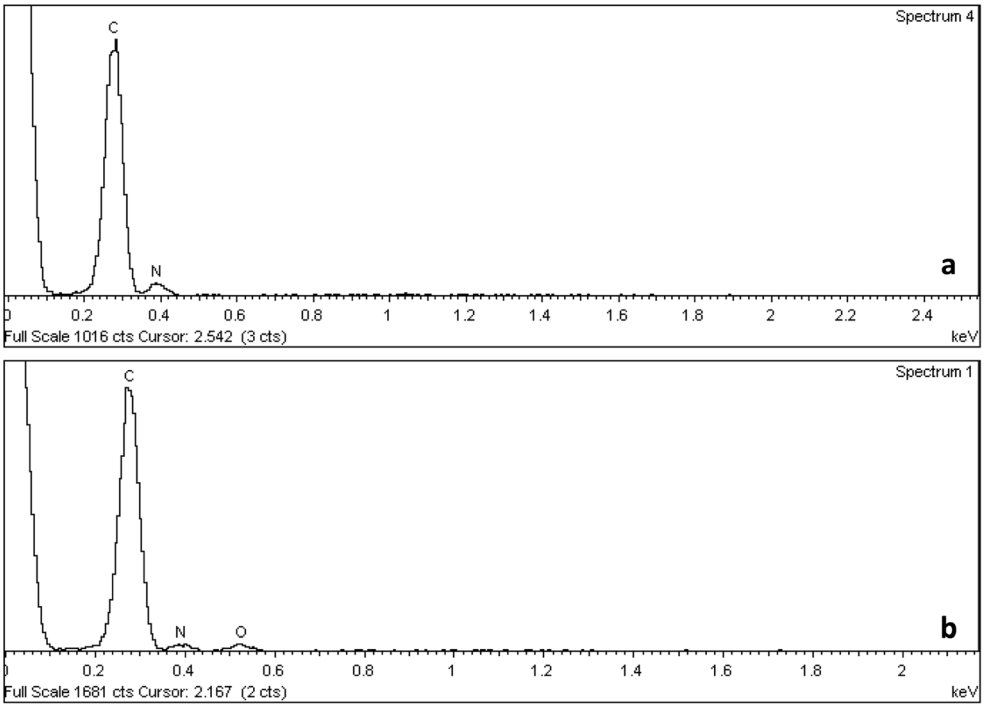

Fig. 2 EDS spectrum and chemical composition of MWCNTs-PAN fibers before (a) and after (b) pyrolysis

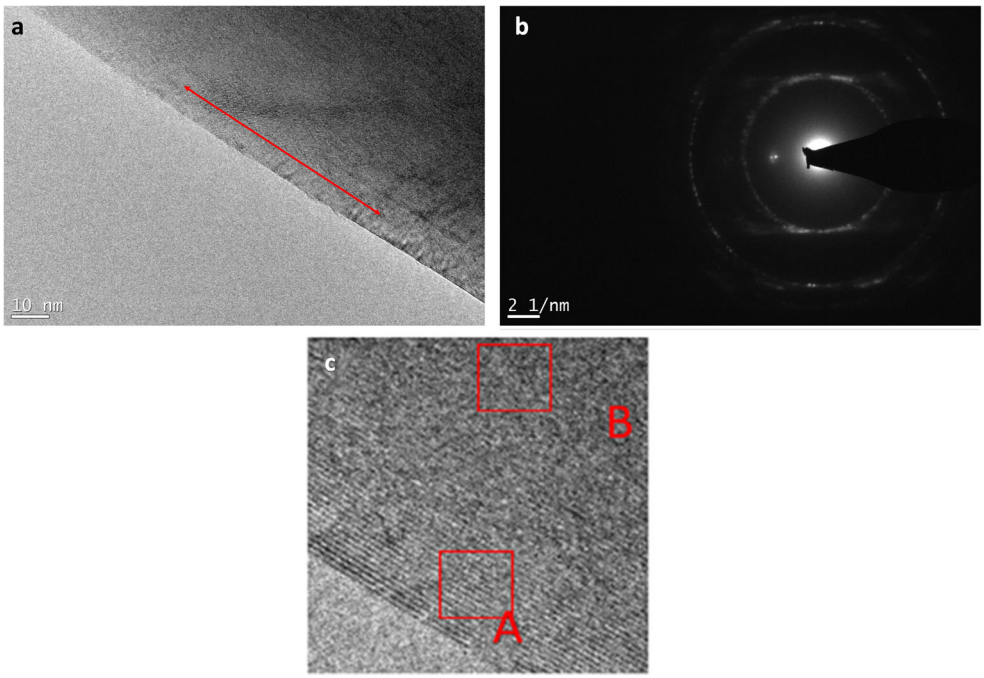

Fig. 3 Bright field images of the MWCNTs-PAN samples (a, b). Detail of the microstructure of the MWCNTs-PAN nanofiber (c)

indicates the distance between the different layers. The average crystallite thickness L_c resulted in 15.1 ± 4.9 nm.

In particular, PAN is a non-graphitized polymer and the structure of the pyrolyzed PAN is indeed disordered and randomly curled [18]. In this case, the MWCNTs-PAN samples exhibit aligned carbon fringes stacked together and generally well-oriented especially on the shell region of the fibers while the graphene planes become imperfect in the core region of the electrospun fibers. With the addition of CNTs, the nanostructure of pyrolyzed PAN fibers appears more graphitic.

RAMAN spectroscopy allows the quantification of the degree and the uniformity of graphitization of the material. The positions, shapes, and intensities of the RAMAN peaks can provide fundamental information about the structural characteristics of the carbon fibers. Three spectra were acquired and averaged across each replica to evaluate the graphitic quality of the resulting carbons. The typical RAMAN spectrum ($\lambda_{excitation} = 532$ nm) collected across the electrospun MWCNTs-PAN carbon fibers is shown in Fig. 4.

The G peak, centered on 1560–1610 cm^{-1}, is related to the in-plane vibrations of pairs of sp^2 hybridized carbon atoms. The reason for this is that graphite is composed of sp^2-bonded carbon in planar sheets in which the bond energy of the sp^2 bonds pushes the vibrational frequency of the bonds and hence the frequency of the band in the Raman spectrum. As a result, the intensity and sharpness of the G peaks are signifying the presence of crystalline graphitic phase in the synthesized material. The D peak at 1300–1400 cm^{-1} is related to the deviation from a perfect graphitic microstructure and thus indicates the level of disorder in graphitic sp^2 structures. The nature of this peak is related to one-phonon elastic scattering and it is interpreted as a measure of the quantity of sp^3 or dangling sp^2 bonds that are causing structural disorders. In this case, the prominent D band in relation to the G band can be attributed to the MWCNTs, given the multi-layer configuration, and indicates a certain degree of disorder in the structure.

The quality of graphitization can be evaluated by the D/G peaks ratio. In particular, a low D/G ratio corresponds to a high level of graphitization within the carbon. Moreover, a uniform RAMAN mapping of the carbon fibers is related to an enhanced graphitization throughout the nanofibrous mats. From Fig. 4, it is possible to see that MWCNTs-PAN samples present a G-peak higher than the D-peak and it can be seen that in certain points, the value of D/G ratio is around 0.5: this means that the presence of MWCNTs helps the graphitization, raising the intensity of G-peak, and the order of the carbon phase, lowering the D-peak. On the other hand, the typical G′ peak (> 2600 cm^{-1}) is not visible in the graph, reasonably due to the overlapped multilayers of disordered graphene and possible oxygenated functional groups. In fact, the G′ peak corresponds to a two-phonon band allowed in the second-order Raman spectra of graphene without any kind of disorder or defects [31].

2.2 Single square vs multiple plates collector

The samples MWCNTs-PAN-SQ and MWCNTs-PAN-MP differs according to the collector used during the electrospinning for each sample: MWCNTs-PAN-SQ is

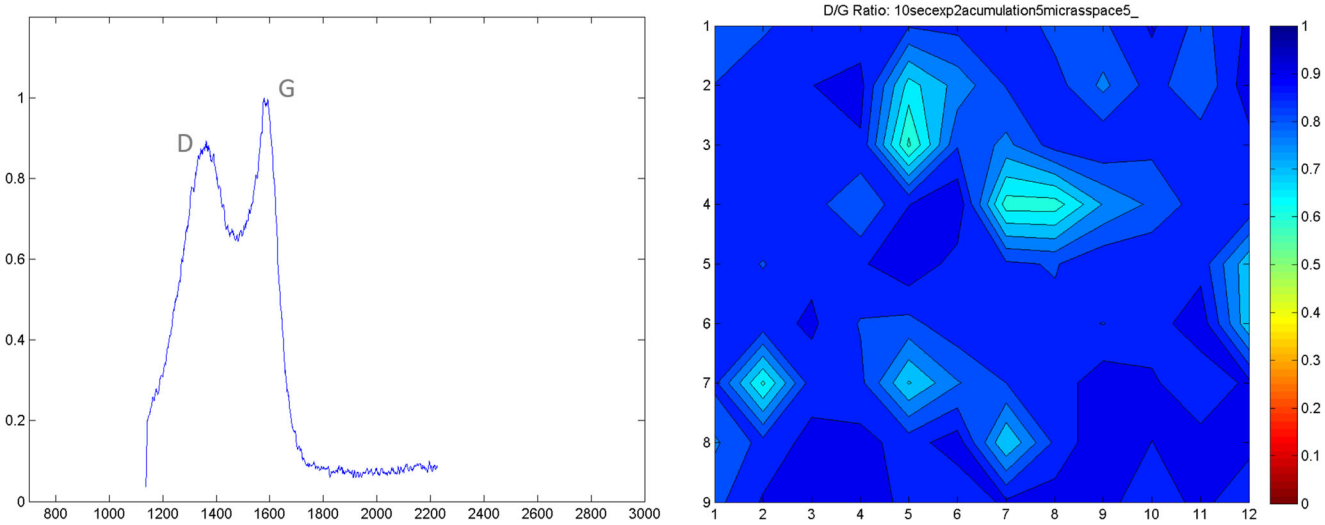

Fig. 4 RAMAN spectrum and D/G ratio mapping of MWCNTs-PAN fibers

obtained with the square collector; MWCNTs-PAN-MP is obtained with the multi-plates collector (Fig. 5).

Hence, the sample MWCNTs-PAN-SQ shows randomly oriented fibers (Fig. 6a) and the sample MWCNTs-PAN-MP shows fibers oriented in a preferential direction (Fig. 6b). The direction of the alignment corresponds to the normal direction to the axes of the plates.

3 Stress induction during thermal stabilization

The precursor carbon fibers are thermally stabilized under ambient air pressure to acquire infusible and nonburning characteristics prior to the carbonization stage. During the thermal stabilization stage, the PAN-CNTs fibers are characterized by a reduction in fiber diameter together with color changes from white to reddish brown [32]. Since the application of mechanical tension during the thermal stabilization is crucial in order to prevent the polymer chains from relaxing and losing their orientation, two ways of mechanical stretching of samples were designed for each sample. Firstly, a compression stress has been applied to the mats and then a tensile stress was chosen to evaluate the effects of this stress on aligned fibers. To allow the application of a compression stress, the MWCNTs-PAN-SQ and MWCNTs-PAN-MP fibrous mats were detached from the collectors and placed between two washers maintained by two clamps to obtain a compression of 15% (Fig. 7a). On the other hand, the MWCNTs-PAN-MP fibrous mats were also subjected to a uniaxial tensile stress applied by a vise to obtain an elongation of 20% in the longitudinal direction (Fig. 7b).

A summary of the experimental tests and applied conditions is reported in Table 1.

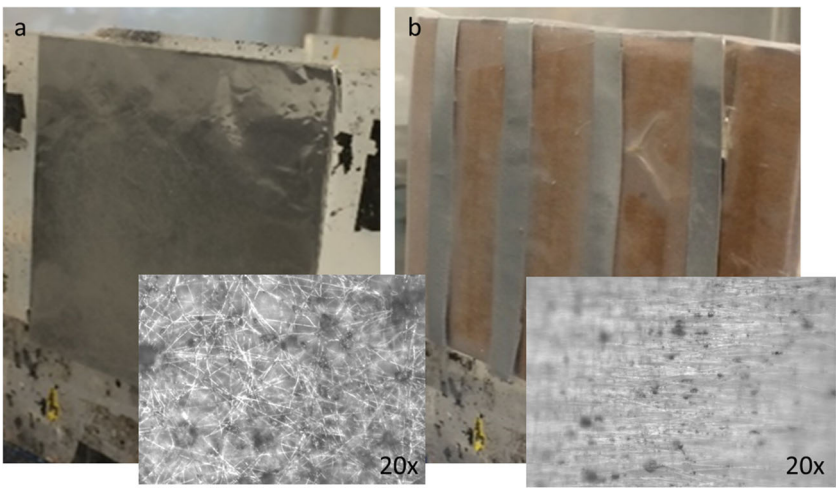

Fig. 5 Square (a) and multi-plates (b) collectors. The insets of the lower corners show the optical microscope images of the as electrospun MWCNTs-PAN fibers on the square and multi-plates collectors

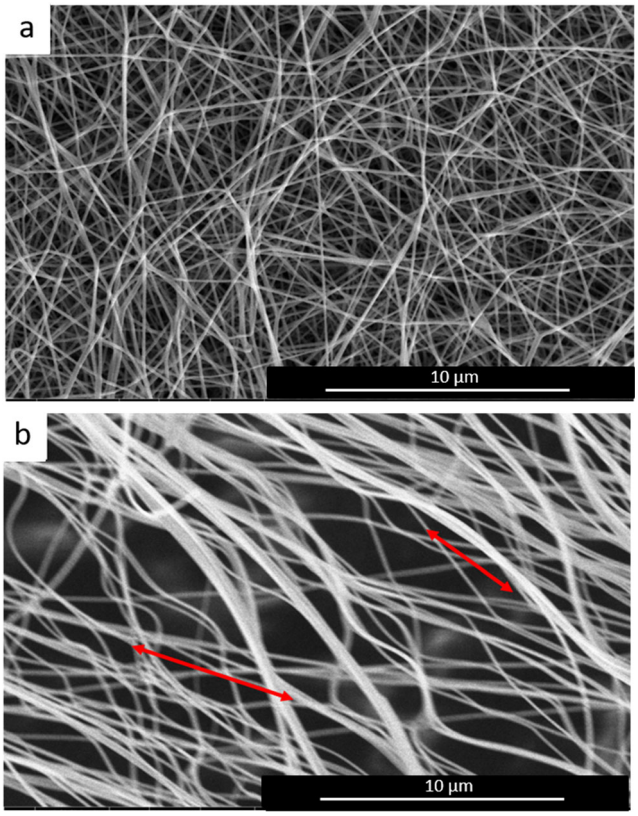

Fig. 6 SEM images of MWCNTs-PAN-SQ (a) and MWCNTs-PAN-MP (b) fibers. The average diameter of the fibers is 132.2 ± 15 nm (porosity = 5.03%) for the MWCNTs-PAN-SQ sample and 169.2 ± 40 nm (porosity = 21%) for MWCNTs-PAN-MP sample

3.1 Compression stress application effects: single square collector

Three samples of MWCNTs-PAN-SQ fibers randomly oriented on the square collector were subjected to a compressive stress during the thermal stabilization prior to pyrolysis and then pyrolyzed. The comparison between unstressed MWCNTs-PAN-SQ and stressed MWCNTs-PAN-SQ-CS fibers is reported in Fig. 8 (SEM) and Fig. 9 (RAMAN).

As shown in Fig. 8, the compression does not affect the orientation of the fibers. It is possible to conclude that the applied load is not causing a re-orientation of the fiber.

Table 1 Summary of the electrospun mats subjected to stress-induced thermal stabilization

Test name	Collector	Applied stress
MWCNTs-PAN-SQ-CS	Square	Compression
MWCNTs-PAN-MP-CS	Multi-plates	Compression
MWCNTs-PAN-MP-E	Multi-plates	Tensile

Thus, the fundamental supramolecular structure of the PAN nanofibers is established during the electrospinning process.

Figure 9 presents the RAMAN shifts for a specific point of the samples MWCNTs-PAN-SQ and MWCNTs-PAN-SQ-CS.

In both the spectra, the D-peak and the G-peak are present. The G-peak is higher than the D-peak in both the samples due to the presence of MWCNTs in the mat, but in the MWCNTs-PAN-SQ-CS sample, the D-peak is lower than the D-peak of the sample MWCNTs-PAN-SQ. This may depend on the mechanical treatment at which sample MWCNTs-PAN-SQ-CS is subjected during stabilization: the applied stress prevents the polymer chains from relaxing and losing their orientation. That means that the microstructure is more ordered: the D-peak lowers and the G′ peak is clearly visible on the spectrum. The reduction of the intensity of the disorder-associated peak reveals a possible increase in the graphitic structure of the mechanically treated samples. Moreover, broader RAMAN peaks are related with a higher level of disorder and defects in the graphitic material. In this case, it is possible to remark a reduction of the areas of both G and D peaks.

Figure 10 shows that the average value of the D/G ratio of sample MWCNTs-PAN-SQ (0.5) is lower than the one of sample MWCNTs-PAN-SQ-CS, but the punctual value of D/G ratio reaches lower values in sample MWCNTs-PAN-SQ-CS. This effect can be attributed to the application of a mechanical tension during stabilization that can enhance the microstructural order of the fibers. The average D/G ratio for sample MWCNTs-PAN-SQ-CS is around 0.8 (ranging from 0.6 to 1). This value can be attributed to an incomplete dispersion of the MWCNTs in the polymer solution.

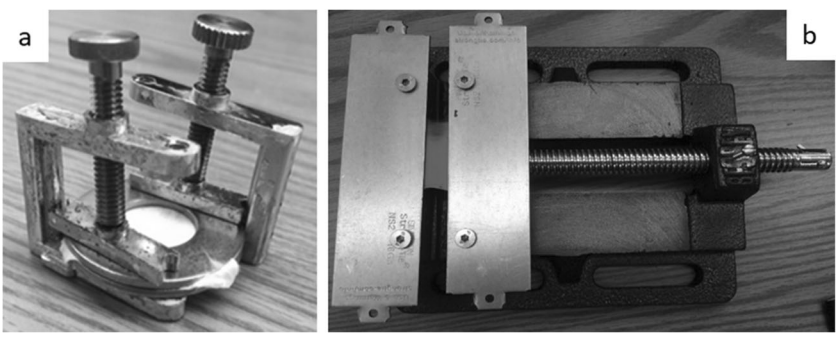

Fig. 7 Washers for the application of the compression stress (a) and vise for the application of the uniaxial tensile stress (b)

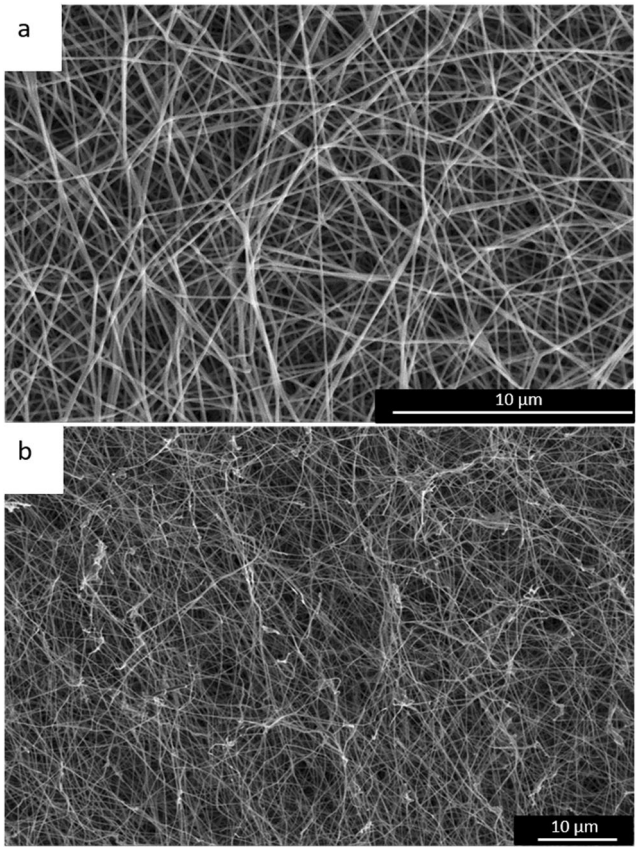

Fig. 8 Comparison between SEM images of MWCNTs-PAN-SQ (a) and MWCNTs-PAN-SQ-CS (b) fibers. The average diameter of the fibers is 132.2 ± 15 nm (porosity = 5.03%) for the MWCNTs-PAN-SQ sample and 168 ± 30 nm (porosity = 4.38%) for MWCNTs-PAN-SQ-CS sample

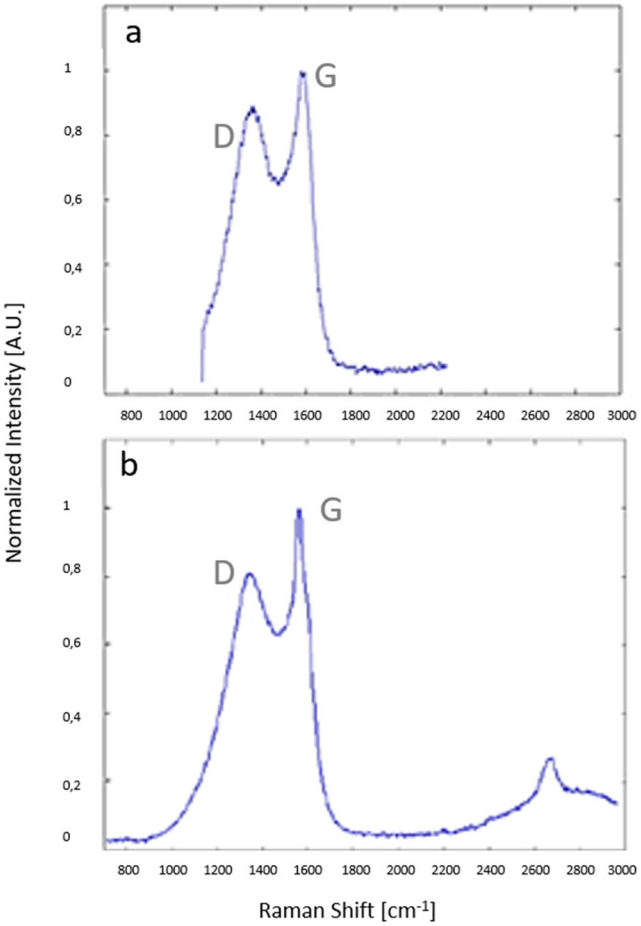

Fig. 9 Comparison between RAMAN spectra of MWCNTs-PAN-SQ (a) and MWCNTs-PAN-SQ-CS (b) fibers

3.2 Compression stress application effects: multiple plates collector

Three samples of MWCNTs-PAN-MP fibers deposited on the multi-plates collector were subjected to the compressive stress during the thermal stabilization prior to pyrolysis and then pyrolyzed. As shown in Fig. 9, the compression seems enhancing the orientation of the MWCNTs-PAN-MP-CS fibers accordingly to their direction given by the multi-plates collector (Fig. 11).

It can be concluded that the application of a compression stress is more effective on the already oriented fibers collected on the multi-plates configuration.

The RAMAN spectrum in Fig. 12 shows similar D and G peak intensities compared to the spectrum in Fig. 9b indicating that the compressive stress is not influencing the degree of graphitization of the fibers in relation to their orientation.

Considering the mapping of sample MWCNTs-PAN-MP-CS, reported in Fig. 12, the average value of D/G ratio results to 0.6 ranging from 0.2 to 0.8. As the stress is uniform on the mat, it is possible to consider the D peak constant and thus that the lowest values of D/G ratio are found in correspondence to the MWCNTs that raise the G-peak.

The average value of the D/G ratio is lower in the MWCNTs-PAN-MP-CS sample if compared to the one related to the MWCNTs-PAN-SQ-CS sample. This local reduction of the D/G ratio can be attributed to the enhanced alignment of the fibers that gives more orientation to the microstructure of the MWCNTs-PAN composite helping the increase of the graphitization degree.

3.3 Compression vs tensile stress: multiple plates collector

Considering the results of the application of the compression stress on the aligned fibers, a controlled vise was used to subject the MWCNTs-PAN-MP fibrous mats to an elongation of $\mathcal{E} = 20\%$.

Figure 13 shows that the sample MWCNTs-PAN-MP-E presents a similar orientation of the fibers compared to the MWCNTs-PAN-MP-CS sample but in this case, it can be seen that the stretching in sample MWCNTs-PAN-MP-E induces more tension on the fibers. The applied tension causes more stress along the fibers' axes resulting in shorter fibers and randomly distributed cracks. Figure 13c reports the transition

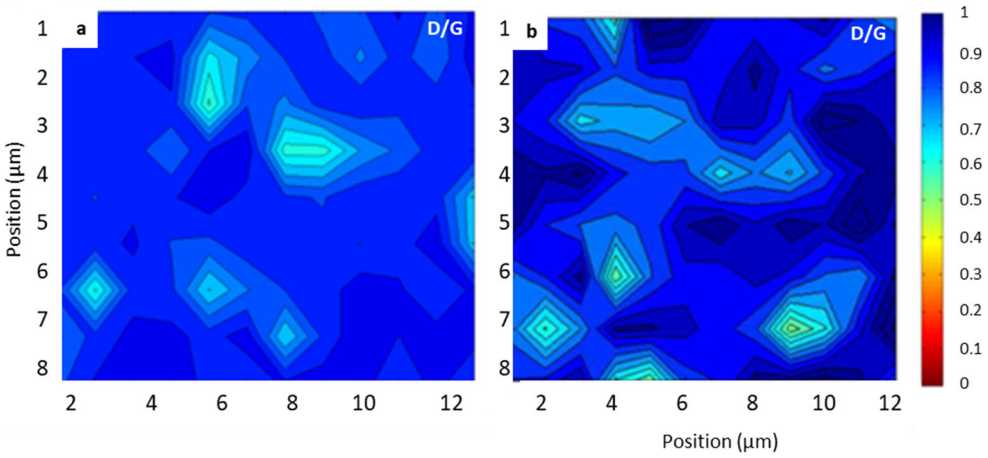

Fig. 10 Comparison between the D/G ratio mapping of MWCNTs-PAN-SQ (a) and MWCNTs-PAN-SQ-CS (b) fibers

of the MWCNTs-PAN fibers from an amorphous nanostructure to a graphitic material with directionally aligned carbon fringes visible on both the shell and core regions of the fiber. In particular, the mechanical tension induced the ordering of the tortuous and randomly oriented carbon planes that became parallel and well-aligned.

In this case, the RAMAN spectrum appears different compared to all the previous conditions. The G-peak intensity, which is affected from the presence of MWCNTs, has the same value of the sample MWCNTs-PAN-MP-CS because the percentage of MWCNTs is the same in both the samples. On the other hand, the G peak area is markedly reduced and

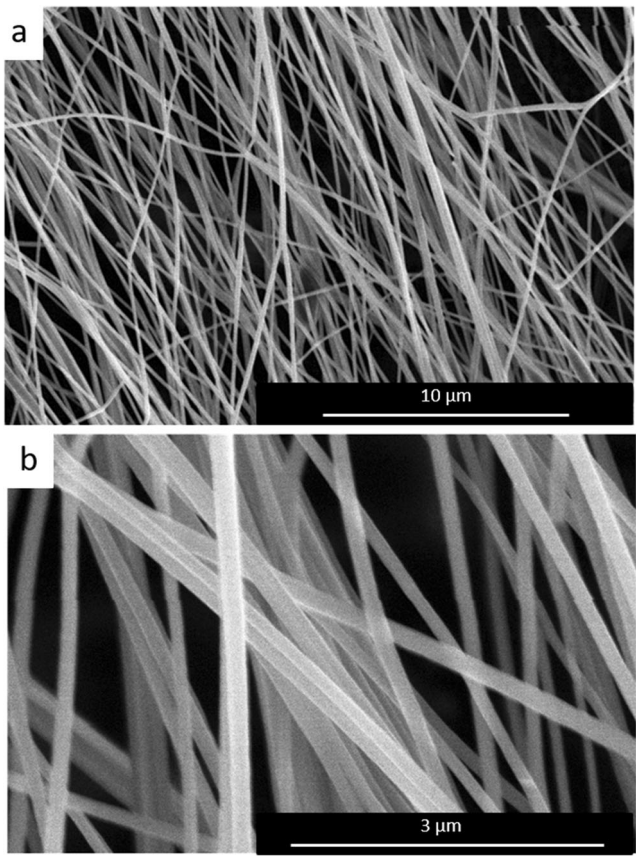

Fig. 11 Lower (a) and higher (b) magnification SEM images of MWCNTs-PAN-MP-CS fibers. The average diameter of the fibers is 159 ± 39 nm (porosity = 19.8%)

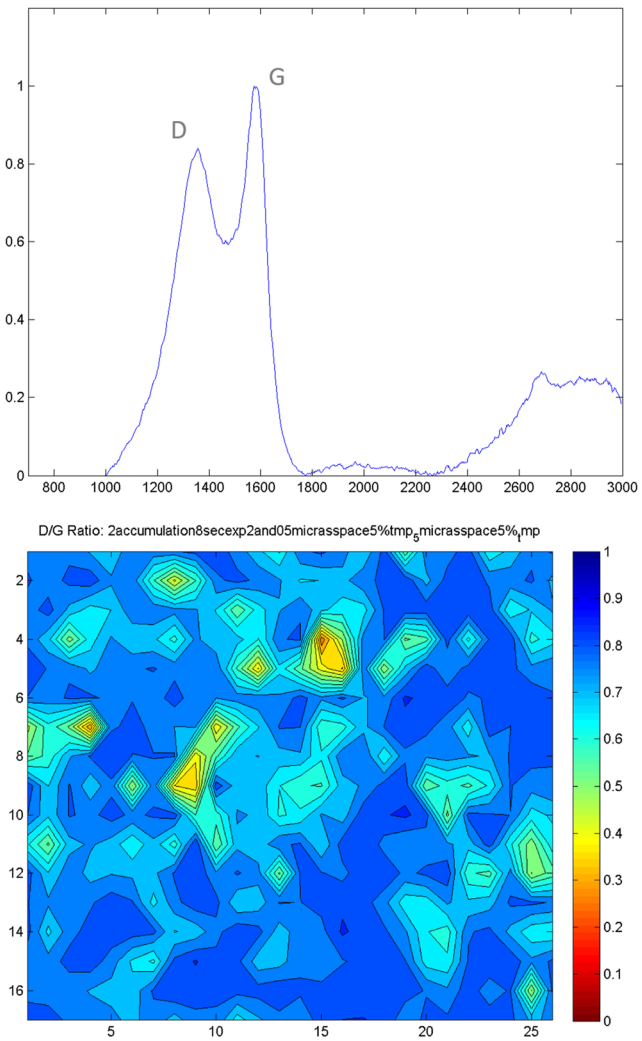

Fig. 12 RAMAN spectrum and D/G ratio mapping of MWCNTs-PAN-MP-CS

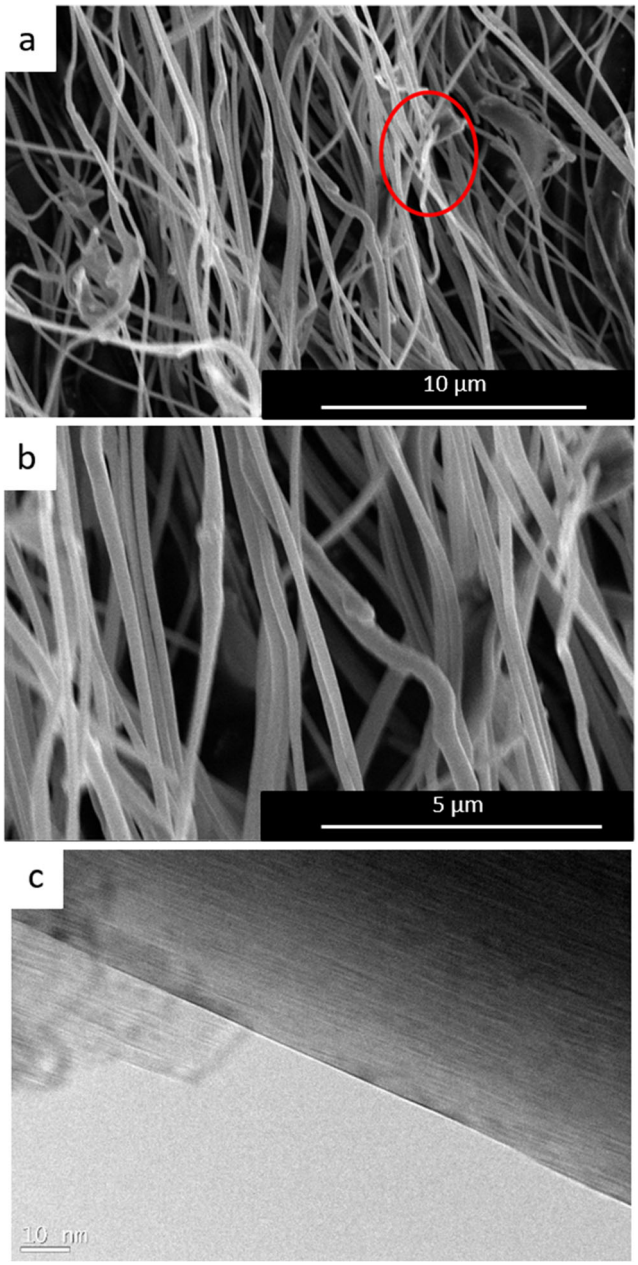

Fig. 13 Lower (a) and higher (b) magnification SEM images of MWCNTs-PAN fibers. The average diameter of the fibers is 183 ± 32 nm (porosity = 16.9%). Bright field images of the MWCNTs-PAN-MP-E samples (c)

the D-peak is abruptly lowered due to the tensile tension applied during stabilization that seems to help lower the microstructural disorder. The sharpness of the G peak is indicating that the bonds are more uniform due to the formation of relatively larger nanocrystallines with the mechanical treatment. Both the evolution of the areas of the G and D peaks and the lowered intensity of the D peak are indicating a substantial reduction of the level of disorder and an increase of the graphitization degree. Moreover, the G′ peak intensity is still lower than the G peak intensity, but the G′ peak increase is probably attributed to the higher stacking order of the graphene layers. The G′ peak shift in graphite (2700 cm^{-1}) is a result of interactions between the stacked graphene layers which result in a tendency to shift the bands to higher frequency (Fig. 14).

The average D/G ratio value for the MWCNTs-PAN-MP-E sample is 0.4 ranging from 0.1 to 0.7. The difference between the ratios observed for the MWCNTs-PAN-MP-CS sample leads on the high difference between the D peak values that in this case is lower due to the application of a different stress state.

From these results, it is possible to conclude that the typical crosslinking phase of precursors occurring when heated to 300 °C is partially followed by a fusion phase in which the molecular structure is not totally fixed and the carbon atoms can rearrange themselves allowing the formation of graphitic planes that are more thermodynamically stable [33]. The results highlighted that the use of CNTs is not modifying the graphitization of the carbon fibers obtained by the pyrolysis of the PAN. On the other hand, the graphitization degree can be

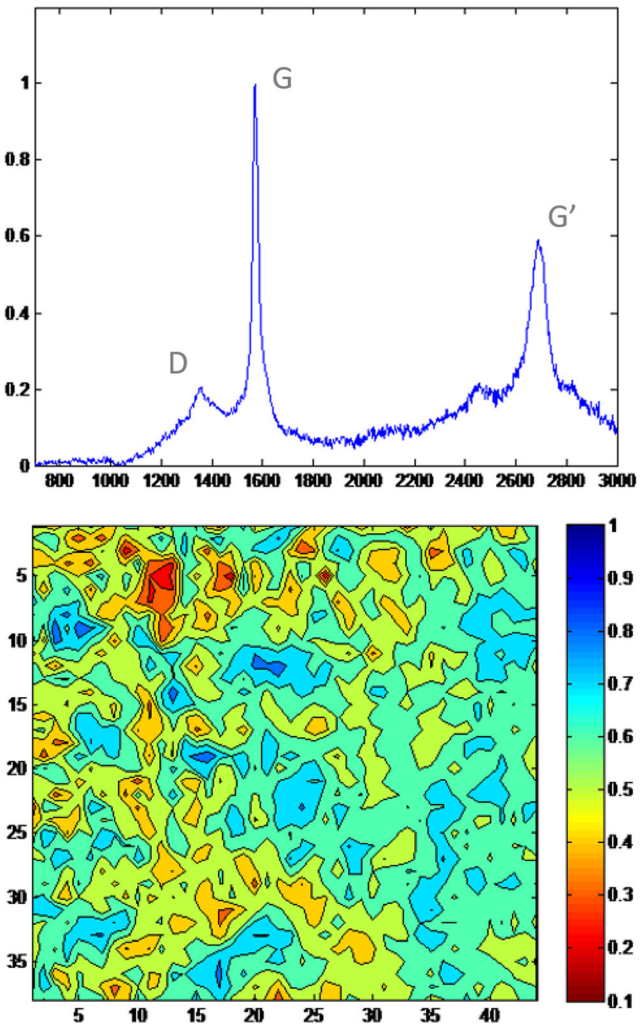

Fig. 14 RAMAN spectrum and D/G ratio mapping of MWCNTs-PAN-MP-E

enhanced by the implementation of a mechanical treatment in the direction of the alignment of the electrospun fibers that causes the reduction of the relative intensity of disorder of the graphitic material.

4 Conclusion and future trends

This paper reports the characterization of carbon fibers derived from the pyrolysis of PAN precursor electrospun fibers. A certain percentage of MWCNTs was added to the polymer solution to study the effects of the presence of nanoparticles on the final orientation and graphitization of the pyrolyzed fibers. The aim was to understand whether PAN fibers may be graphitized at lower pyrolysis temperature compared to the current commercial processes followed for graphitizing polymers [16].

The results show that a multi-plates configuration of the collector can lead to a preferential direction of the fibers but has no effects on the degree of graphitization of the fibers. The MWCNTs-PAN-aligned fibers were subjected to a compression load equally distributed on the fibrous mats to try to preserve the polymer chain alignment. In this case, the D/G ratio mapping showed an interesting difference compared to the previous results, indicating a lower degree of disorder of the carbon phase within the fibers. A tensile stress was then applied to the MWCNTs-PAN aligned fibers and the SEM images showed that the stressed fibers maintained their orientation despite of an over tension state effect occurred due to the stretching. In this final case, the RAMAN spectrum and D/G ratio mapping showed remarkable differences compared to the previous results. It can be concluded that, in this case, a lower disorder degree of the carbon phase of the pyrolyzed MWCNTs-PAN fibers, and subsequently, a higher degree of graphitization, was achieved. These results on the pyrolyzed fibers properties indicate that it is possible to tailor the carbon fibers microstructure according to the specific requirements. In particular, this analysis demonstrates that the graphitization of PAN-derived carbon fibers can be correlated to the conditions imposed during the stabilization of the precursor polymer. The combination of electrospinning, addition of carbon nanotubes and mechanical tension applied has been demonstrated to promote the molecular rearrangement during the heat treatment of PAN precursor enhancing its graphitization at reduced pyrolysis temperature. In particular, the MWCNTs added to the PAN solution influence the dielectrophoretic forces during the electrospinning process producing an alignment of the polymer molecular chains. Although the graphitization of organic precursors is a complex mechanism that still needs to be fully understood, this work demonstrates that the treatments applied can have a strong influence on the microstructures of a polymer turned into graphitic carbon providing a promising route to explore new applications of the graphitization of PAN electrospun fibers. Accordingly, the future research will be focused on the study of the electrochemical performances of electrospun structures made of pyrolyzed MWCNTs-PAN fibers for sensing and tissue engineering applications. In particular, the response of the treated PAN-MWCNTs seems to be increased both as hydrogen peroxide and iodine sensors as well as when applied for electrochemical sensing platforms without requiring additional post-processing to functionalize the carbon electrodes [34].

Acknowledgments The authors would like to acknowledge the support and the assistance of Prof. Marc Madou, Dr. Sunny Holmberg, Dr. Arnoldo Salazar at University of California Irvine and the technical assistance of Dr. Michele Norbis.

References

1. Ginestra P, Ceretti E, Fiorentino A (2016) Electrospinning of polycaprolactone for scaffold manufacturing: experimental investigation on the process parameters influence. Procedia CIRP 49:8–13
2. Ginestra P, Fiorentino A, Ceretti E (2017) Micro-structuring of titanium collectors by laser ablation technique: a novel approach to produce micro-patterned scaffolds for tissue engineering applications. Procedia CIRP 65:19–24
3. Ginestra P, Pandini S, Fiorentino A, Benzoni P, Dell'Era P, Ceretti E (2017) Microstructured scaffold for cellular guided orientation: PCL electrospinning on laser ablated titanium collector. CIRP JMST 19:147–157
4. Zhu Z, Garcia-Gancedo L, Flewitt AJ, Xie H, Moussy F, Milne WI (2012) A critical review of glucose biosensors based on carbon nanomaterials: carbon nanotubes and graphene. Sensors 12:5996–6022
5. Pollack B, Holmberg S, George D, Tran I, Madou M, Ghazinejad M (2017) Nitrogenrich polyacrylonitrile-based graphitic carbons for hydrogen peroxide sensing. Sensors 17:2407
6. Bisht GS, Canton G, Mirsepassi A, Kulinsky L, Oh S, Dunn-Rankin D, Madou M (2011) Controlled continuous pattering of polymeric nanofibers on three-dimensional substrates using low-voltage near-field electrospinning. Nano Lett 11:1831–1837
7. Arshad SN, Naraghi M, Chasiotis I (2011) Strong carbon nanofibers from electrospun polyacrylonitrile. Carbon 49:1710–1719
8. Ra EJ, An KH, Kim KK, Jeong SJ, Lee YH (2015) Anisotropic electrical conductivity of MWCNT/PAN nanofiber paper. Chem Phys Lett 416:188–193
9. Dumanlı AG, Windle AH (2012) Carbon fibers from cellulosic precursors: a review. J Mater Sci 47:4236–4250
10. Yusof N, Ismail AF (2012) Post spinning and pyrolysis process of polyacrylonitrile (PAN)- based carbon fiber and activated carbon fiber: a review. J Anal App Pyrolysis 93:1–13
11. Singh A, Jayaram J, Madou M, Akbar S (2012) Pyrolysis of negative photoresists to fabricate carbon structures for microelectromechanical systems and electrochemical applications. J Electrochem Soc 149:E78–E83
12. Pumera M (2013) Electrochemistry of graphene, graphene oxide and other graphenoids: review. Electrochem Commun 36:14–18
13. Hiremath N, Mays J, Bhat G (2016) Recent developments in carbon fibers and carbon nanotube-based fibers: a review. Pol Rev 57:339–368
14. Hiremath N, Evora MC, Naskar AK, Mays J, Bhat G (2017) Polyacrylonitrile nanocomposite fibers from acrylonitrile-grafted carbon nanofibers. Composite Part B: Engineering 130:64–69

15. Prilutsky S, Zussman E, Cohen Y (2018) The effect of embedded carbon nanotubes on the morphological evolution during the carbonization of poly(acrylonitrile) nanofibers. Nanotechnology 19: 165603
16. Toray Innovation by Chemistry. http://www.torayca.com
17. Mathur RB, Bahl OP, Dhami TL, Chauhan SK (2003) A novel route to realise high degree of graphitization in carbon-carbon composites derived from hard carbons. Carbon Science 4(3):111–116
18. Holmberg S, Ghazinejad M, Cho E, George D, Pollack B, Perebikovsky A, Ragan R, Madou M (2018) Stress-activated pyrolytic carbon nanofibers for electrochemical platforms. Electrochmica Acta 290:639–648
19. Maitra T, Sharma S, Srivastava A, Cho YK, Madou M, Sharma A (2012) Improved graphitization and electrical conductivity of suspended carbon nanofibers derived from carbon nanotube/ polyacrylonitrile composites by directed electrospinning. Carbon 50: 1753–1761
20. Qiao B, Ding X, Hou X, Wu S (2011) Study on the electrospun CNTs/polyacrylonitrile-based nanofiber composites. J Nanomater. https://doi.org/10.1155/2011/839462
21. Caia J, Chawlab S, Naraghi M (2016) Microstructural evolution and mechanics of hot-drawn CNT-reinforced polymeric nanofibers. Carbon 109:813–822
22. Shirvanimoghaddam K, Abolhasani MM, Li Q, Khayyam H, Minoo N (2017) Cheetah skin structure: a new approach for carbon-nano-patterning of carbon nanotubes composites part a applied science and manufacturing. https://doi.org/10.1016/j.compositesa.2017.01.023
23. Li X, Qin A, Zhao X, Liu D, Wang H, He C (2015) Drawing dependent structures, mechanical properties and cyclization behaviors of polyacrylonitrile and polyacrylonitrile/carbon nanotube composite fibers prepared by plasticized spinning. Phys Chem 17: 21856–21865
24. Ginestra PS, Ghazinejad M, Madou M, Ceretti E (2016) Fabrication and characterization of polycaprolactone-graphene powder electrospun nanofibers. Proceeding of SPIE 9932 carbon nanotubes graphene and emerging 2D materials for electronic and photonic devices IX 99320A
25. Ceretti E, Ginestra PS, Ghazinejad M, Fiorentino A, Madou M (2017) Electrospinning and characterization of polymer-graphene powder scaffolds. CIRP Ann 66(1):233–236
26. Chen R, Liu J, Sun Z, Chen D (2018) Functional Nanofibers with multiscale structure by electrospinning. Nanofabrication 4:17–31
27. Ulubayram K, Calamak S, Shahbazi R, Eroglu I (2015) Nanofibers based antibacterial drug design, delivery and applications. Curr Pharm Des 21:1930–1943
28. Ginestra PS, Madou M, Ceretti E (2019) Production of carbonized micro-patterns of photolithography and pyrolysis. Precis Eng 55: 137–143
29. Ghazinejad M, Holmberg S, Pilloni O, Oropeza-Ramos L, Madou M (2017) Graphitizing non-graphitizable carbons by stress-induced routes. Sci Rep 7:16551. https://doi.org/10.1038/s41598-017-16424-z
30. Karacan I, Erdogan G (2012) The role of thermal stabilization on the structure and mechanical properties of polyacrylonitrile precursor fibers. Fibers Polym 13(7):855–863
31. Malard LM, Pimenta MA, Dresselhaus G, Dresselhaus MS (2009) Raman spectroscopy in graphene. Phys Rep 473:51–87
32. Fitzer E, Müller DJ (1975) The influence of oxygen on the chemical reactions during stabilization of pan as carbon fiber precursor. Carbon 13:63–69
33. Kipling JJ, Sherwood JN, Shooter PV, Thompson NR (1964) Factors influencing the graphitization of polymer carbons. Carbon 1:315–320
34. Cho E, Perebikovsky A, Benice O, Holmberg S, Madou M, Ghazinejad M (2018) Rapid iodine sensing on mechanically treated carbon nanofibers. Sensors 18:1486. https://doi.org/10.3390/s18051486